Adsorption (2009) 15: 13–22
DOI 10.1007/s10450-008-9148-3

Behavior of ethylene and ethane within single-walled carbon nanotubes, 2: dynamical properties

Fernando J.A.L. Cruz · Erich A. Müller

Received: 19 March 2008 / Revised: 28 November 2008 / Accepted: 16 December 2008 / Published online: 28 February 2009

Abstract The dynamical behavior of ethylene and ethane confined inside single-walled carbon nanotubes has been studied using Molecular Dynamics and a fully atomistic force field. Simulations were conducted at 300 K in a broad range of molecular densities, $0.026\ \text{mol}\cdot\text{L}^{-1} < \rho < 15.751\ \text{mol}\cdot\text{L}^{-1}(C_2H_4)$ and $0.011\ \text{mol}\cdot\text{L}^{-1} < \rho < 14.055\ \text{mol}\cdot\text{L}^{-1}(C_2H_6)$, and were oriented towards the determination of bulk and confined phase self-diffusion coefficients. In the infinite time limit, Fickian self-diffusion is the dominant mode of transport for the bulk fluids. Upon confinement, there is a density threshold ($\rho = 5.5\ \text{mol}\cdot\text{L}^{-1}$) below which we observe a mixed mode of transport, with contributions from Fickian and ballistic diffusion. Nanotube topology seems to have only a small influence on the confined fluids' dynamical properties; instead density (loading capacity) assumes the dominant role. In all cases studied and at a given density, the diffusivities of ethylene are larger than those of ethane, although the difference is relatively minor. We note the collapse of self-diffusivities obtained from the bulk fluids and confined phases into a unique single trend. These results suggest that it might be possible to infer dynamical properties of confined fluids from the knowledge of their bulk phase densities.

Keywords Diffusion · Carbon nanotubes · Ethylene · Ethane · Molecular dynamics

Electronic supplementary material The online version of this article (http://dx.doi.org/10.1007/s10450-008-9148-3) contains supplementary material, which is available to authorized users.

F.J.A.L. Cruz · E.A. Müller (✉)
Department of Chemical Engineering, Imperial College London, South Kensington Campus, London SW7 2AZ, UK
e-mail: e.muller@imperial.ac.uk

1 Introduction

In recent years it has been suggested that single-walled carbon nanotubes (SWCNTs) could be used as active separating sites in membranes (Majumder et al. 2006; Sholl and Johnson 2006; Corry 2009). To efficiently use SWCNTs in such separation devices, it becomes essential not only to study their selectivity/equilibrium properties but also to understand the confined fluids' dynamics. Experimentally, the investigation of the transport properties/diffusion mechanism of nanoconfined fluids is hindered by several aspects including, but not limited to, poor characterization of the samples, lack of description of surface topology, purity of the samples and the small size of confined spaces. In this context, computer simulations can play an important role overcoming the experimental difficulties. Typical applications of molecular simulation in this context include the study of flow and transport properties of binary fluid mixtures through nanoporous carbon membranes, such as O_2/N_2 and CH_4/N_2 (Chen and Sholl 2006; Arora and Sandler 2007). Skoulidas et al. have employed molecular dynamics calculations to study the adsorption and diffusion behavior of pure CO_2 and N_2 inside single-walled carbon nanotubes (Skoulidas et al. 2006). The transport coefficients of light gases confined in SWCNTs, such as CH_4 and H_2, have also been estimated using molecular dynamics calculations (Bhatia et al. 2005). Due to its obvious biological and industrial applications, water diffusion on pristine and decorated CNTs has also become a very active research area (Striolo 2006; Mukherjee et al. 2007; Striolo 2007; Alexiadis and Kassinos 2008). A common practice whenever adsorption and diffusion properties need to be addressed is to use Monte Carlo simulations to determine the adsorption characteristics, and complement those results with dynamical information obtained with molecular dy-

namics simulations (Düren et al. 2002; Cao and Wu 2004; Krishna and van Baten 2006; Valiullin et al. 2006).

In a previous work, henceforth designated as part I (Cruz and Müller 2008), we have presented detailed computer simulation results on the equilibrium and adsorption properties of C_2H_4 and C_2H_6 and their corresponding binary mixtures, when bulk fluids were put in contact with SWCNTs. Two different force-fields were employed, namely a coarse grained model and a fully atomistic potential. It was shown that both intermolecular potentials exhibit the same features for the adsorption isotherms of pure fluids, but they did not match quantitatively, especially in the vicinity of ambient pressure; as pressure surpassed a threshold ($p \approx 10$ bar), both models would predict the same results. It was also shown that, under the studied thermodynamic conditions, those nanoporous materials exhibited similar selectivities regarding the separation of the corresponding binary mixtures, when compared to idealized slit-pore geometries and larger diameter nanotubes.

It is known that the adsorption of fluids onto nano and mesopores can be accompanied by striking effects on their confined phase dynamics (Rouquerol et al. 1998; Gelb et al. 1999; Coasne et al. 2006), which do not possess an analogy in the bulk phase. An accurate investigation of molecular transport under confinement is therefore of the utmost importance. It can be classified under three main categories, according to the molecular mode of displacement: (1) Fickian or self-diffusive, resulting from the random nature of the particles translational movement, (2) single-file, when molecules are prevented from passing each other as a consequence of their large size relatively to the pore diameter, and (3) ballistic, reflecting a highly coordinated molecular motion mechanism. Transitional and/or intermediate regimes may occur, and their particular characteristics depend on the physical interactions between the confined fluid and the solid wall, but also on the pore loading capacity (Leroy et al. 2004; Dubbeldam et al. 2005). Adopting the hard-sphere potential for a model fluid in narrow cylindrical pores, Mon and Percus (2002) have characterized the dynamical transition from single-file mode to Fickian diffusion; a similar phenomena has been observed in zeolites (Zimmermann et al. 2007), involving a change of the initial ballistic-type displacement to Fickian diffusion.

It is the purpose of this paper to study the diffusion of pure C_2H_4 and C_2H_6 confined inside SWCNTs of different loadings and topologies, using Molecular Dynamics (MD) simulations and a fully atomistic force-field for both the fluids and the nanotubes. As far as the authors are aware there are no reported experimental data for the diffusion properties of ethane and ethylene inside SWCNTs, and only a handful of simulation studies employing less detailed force-fields than ours has been presented in the literature, for C_2H_6 (Mao and Sinnott 2000, 2001, 2002; Krishna and van Baten 2006; Jakobtorweihen et al. 2007) and C_2H_4 (Mao and Sinnott 2000, 2002) In the next section we will introduce the models used in the simulations as well as the structural characteristics of carbon nanotubes. In the subsequent section we will present results from MD calculations, for the bulk and confined fluid phases.

2 Force fields and models

The intermolecular potentials used in the MD simulations have already been thoroughly described in part I of this work (Cruz and Müller 2008), and will be summarized here for completeness. Interactions between particles are modeled employing the all-atom OPLS (AA-OPLS) force-field, with the parameterization given by Jorgensen and co-workers (Jorgensen et al. 1996; McDonald et al. 1997), and considering explicit electrostatic charges. All fluid molecules are modeled as flexible, i.e. bond stretching, angle bending and dihedral energies were explicitly considered. SWCNTs are described in an atomistic way, where carbon atoms are assumed to be a collection of discrete Lennard-Jones spheres, with parameters $\varepsilon = 28.0$ K and $\sigma = 3.4$ Å (Steele 1973, 1974, 1993). The nanotube walls are rigid and corrugated, i.e., all atoms on the wall are explicitly included in the calculations.

Tube flexibility can play an important role when the carbon lattice is allowed to breathe; this can be simulated at the expense of large computer processing time, allowing the atoms in the solid walls to translate in $x - y - z$ space, constrained only by the sigma bonds of the graphitic network. To avoid these complications, Jacobtorweihen et al. (2006, 2007) employed a modified version of the Lowe-Andersen thermostat, enabling them to mimic the breathing of $(13, 0)$ and $(20, 0)$ SWCNTs. They monitored the diffusion of confined n-alkanes, with $n < 6$, and concluded that tube flexibility is only important for the lighter alkanes in the zero-loading limit. In this latter case, their simulations for C_2H_6 resulted in a reduction by half of the corresponding self-diffusion coefficient, when changing from a rigid framework into a flexible one. As for the tube's diameter, it also has an important role to play: in the case of n-butane inside a 10 Å diameter rigid CNT, the corresponding diffusion coefficient decreases by roughly 27% when comparing with the flexible host (Jakobtorweihen et al. 2007). Chen et al. (2006) reached a similar conclusion, and verified that tube breathing was only important when simulations were conducted close to zero pressure, that is, in the limit of zero-loading. An analogous situation can also be found in zeolitic hosts, where Zimmermann et al. (2007) showed that the usage of an inappropriate force field to describe the system's physical properties may lead to larger errors than those arising from assuming a rigid model for the solid phase. Considering all the previous evidences, one is led to expect that for

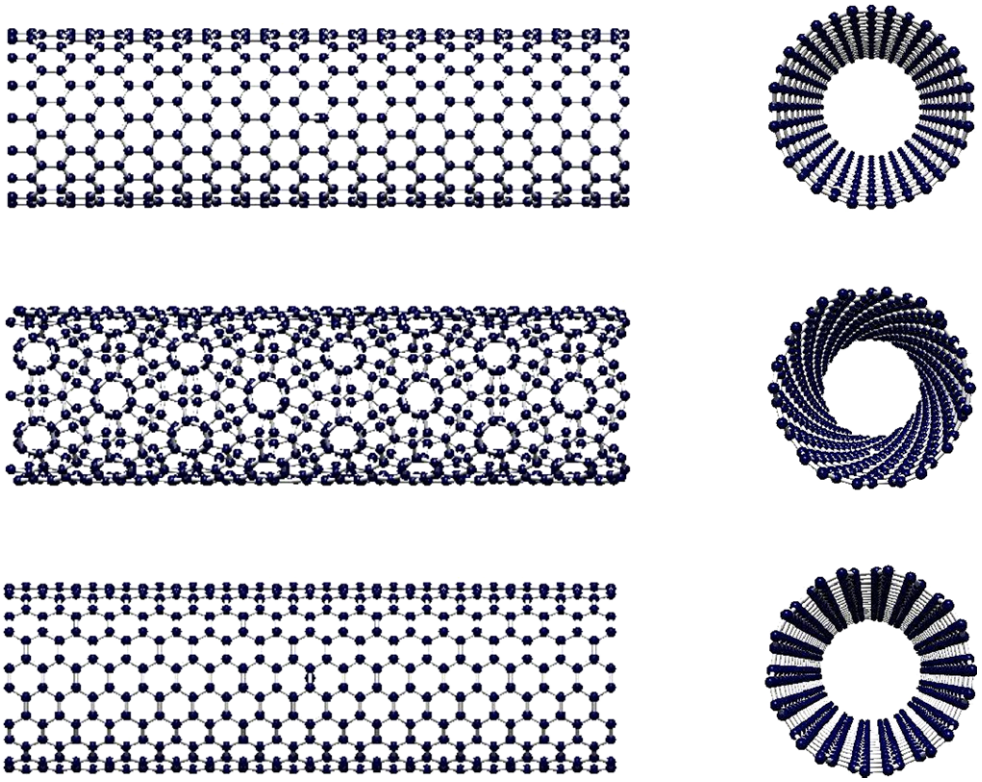

Fig. 1 Single-walled carbon nanotubes along the longitudinal (*left*) and axial (*right*) directions. *From top to bottom*: zig-zag (16, 0), chiral (12, 6) and armchair (10, 10) topologies. Note the evident spiraling alignment of carbon atoms, in the chiral symmetry

simulations away from the zero-loading limit, postulating *a priori* nanotube rigidity would result in only small discrepancies compared with the flexible structure. We have therefore considered rigid nanotube walls, similarly to what has usually been employed by others when studying dynamical properties of confined fluids inside SWCNTs (Cao and Wu 2004; Chen and Sholl 2004, 2006; Krishna and van Baten 2006; Striolo 2007; Alexiadis and Kassinos 2008).

The formation of SWCNTs can be rationalized imagining the bending of a planar graphene sheet to originate a carbon nanotube. This process is accompanied by the squeezing-out of the π clouds towards the nanotube exterior volume (Meyyappan 2005), and the effect will tend to increase the purely sp^2 hybridized σ (C–C) bond, 1.4 Å. In the simulations, we have used a value of 1.42 Å for the C–C sigma bond, in line with our previous work on the adsorption properties of these systems. We have considered three single-walled carbon nanotube structures, with approximately the same effective diameter but with different atomic arrangements (chirality): zig-zag (16, 0), with a diameter (center-center) of 12.55 Å, chiral (12, 6) with a diameter (center-center) of 12.43 Å, and armchair (9, 9) with a diameter (center-center) of 12.18 Å, and a total length, L, of 206 Å (Fig. 1).

We have assumed that the accessible volume that can be occupied by the fluid is given by $D_{eff} = D - \sigma_{CRT}$, where σ_{CRT} is the Lennard-Jones diameter of a graphitic carbon atom (3.4 Å), and D is the nanotube diameter measured from the center of the carbon atoms (Kaneko et al. 1994; Ohba and Kaneko 2002). From this it follows that the internal confining volume used to report our simulation results is given by $V = (\pi/4) \cdot D_{eff}^2 \cdot L$. It should be noted that this diameter corresponds to a rather arbitrary definition of the nanotubes' geometry, however it does not affect in any way the results obtained from molecular simulations.

All the interactions between unlike particles were calculated using cross interaction parameters $(\sigma_{ij}, \varepsilon_{ij})$ according to the classical Lorentz-Berthelot combining rules (Rowlinson and Swinton 1982; Allen and Tildesley 1990), $\sigma_{ij} = (\sigma_{ii} + \sigma_{jj})/2$, $\varepsilon_{ij} = (\varepsilon_{ii} \cdot \varepsilon_{jj})^{1/2}$, and no attempt has been made to adjust them, as no reliable experimental dataset is available.

3 Simulation details

Classical molecular dynamics simulations were performed using the DL_POLY 2.16 package (Smith and Todorov 2006). The Verlet algorithm (Verlet 1967; van Gunsteren and Berendsen 1990) was used to integrate the equations of motion, the long-range electrostatic interactions for the fluids were calculated by the Ewald summation method (Woodcock and Singer 1971; Nosé 1984), and the Nosé-Hoover thermostat was used to control the temperature (Nosé 1984). All MD runs were performed setting the thermostat for $T = 300$ K under the canonical ensemble (*NVT*).

A potential cut-off distance of 15 Å and a time step of $t = 1$ fs were used.

To study the effect on dynamics of fluid confinement, a simulation cell was built from the final configuration of a previous conducted adsorption run (Cruz and Müller 2008); the corresponding volume, containing the (16, 0) zig-zag nanotube and the adsorbed molecules, was separated from the bulk fluid phase and replicated four times along the z-axis to produce a 30 × 30 × 206 Å supercell with 3104 graphitic carbon atoms. To monitor the effect of nanotube chirality on the fluids transport properties, the zig-zag SWCNT was replaced either by a chiral (12, 6) tube or an armchair (9, 9) tube, having, respectively, a total number of graphitic carbon atoms of 3066 and 3006. It should be noted that simulations were run independently from one another, for they always started from different initial configurations. According to the number of confined molecules and the effective pore volume (cf. Sect. 2), fluid molecular densities inside the tubes ranged from 0.242 mol·L^{-1} $< \rho <$ 15.751 mol·L^{-1} and 0.242 mol·L^{-1} $< \rho <$ 14.055 mol·L^{-1}, for ethylene and ethane, respectively. In order to establish a comparison with the bulk fluid phases, we have also studied a simulation box of 30 × 30 × 250 Å without the nanotube, i.e., containing only the bulk fluid, with densities ranging from 0.026 mol·L^{-1} $< \rho <$ 2.969 mol·L^{-1} (C_2H_4) and 0.011 mol·L^{-1} $< \rho <$ 3.711 mol·L^{-1} (C_2H_6). In both the bulk and confined fluid phases, MD simulations were run up to a total time length of 500 ps, and the corresponding data have been used to study the mode of molecular displacement. The sequence of configurations stored in the output files was used to determine the mean-squared displacement (MSD) along the total available pore volume as a function of simulation time, considering at least 100 ps of simulation data. In order to achieve statistically significant results, we used small delay times between origins (Haile 1992): 2495 origins, separated by 1 ps, and calculations were performed over all molecules in the system.

We have taken care when running simulations at (or close to) the limit of infinite dilution. Theoretically, one would insert only a single particle in the nanotube and study its behavior, but at such low density, however, molecular simulations can result in poor statistics. The common practice (Dubbeldam et al. 2005) to avoid such difficulties is to insert a very small number of particles in the simulation box, corresponding to the low-density limit, where effectively adsorbed fluid particles do not interact with each other. Zimmermann et al. (2007) conducted twenty independent simulations containing only one methane molecule and compared their findings with a set of five simulations containing 64 ideal molecules; results point out to a discrepancy of less than 3% in the averaged diffusivities. In the present work, we have used two molecules of either C_2H_4 or C_2H_6 in the lowest density confining boxes.

4 Results

When molecules move according to a total random behavior, the corresponding self-diffusion coefficient (or Fickian self-diffusivity), D, relates the molecular mean-squared displacement, $MSD = \langle [r(t) - r(0)]^2 \rangle$, to the observation time, t, via Einstein's relation (Eq. 1) (Allen and Tildesley 1990; Haile 1992), where r is the positional vector in the $x - y - z$ space. Other modes of transport can coexist along with Fickian diffusion, when molecules cease to move randomly. In this case we can still determine a mobility coefficient, as a proportionality constant between $\langle r^2 \rangle$ and observation time: according to that relationship, it is referred to as single-file, $\langle r^2 \rangle \propto F\mathrm{d}t^{1/2}$, or ballistic transport, $\langle r^2 \rangle \propto B\mathrm{d}t^2$ (Fig. 2)

$$D = \frac{1}{6}\frac{\mathrm{d}}{\mathrm{d}t}\langle [r(t) - r(0)]^2 \rangle. \tag{1}$$

Discrimination between the three different modes of transport usually involves long simulation times, ideally in the infinite time limit. Transient behavior can be observed for small time lengths, and this is particularly relevant in the case of confined fluids; for bulk phases, this intermediate behavior usually takes place in quite short time lengths (Striolo et al. 2005). In the subsequent discussion where we report the results, self-diffusion coefficients have been calculated after an initial period of 100 ps (except where clearly mentioned). This "equilibration" period is similar to the whole time length of previous simulations carried out on systems identical to ours (Mao and Sinnott 2000). Probably because of this, the reported dynamical transition between single-file and Fickian self-diffusion for ethane on a (16, 0) SWCNT has not been observed in our studies. Interestingly, despite the relatively narrow tube diameters used in our simulations,

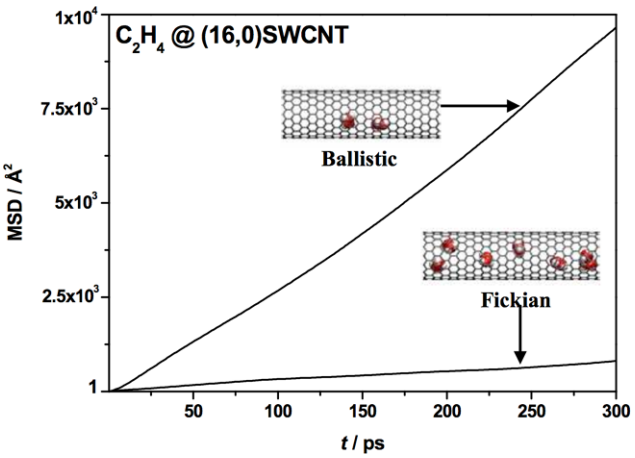

Fig. 2 Different modes of transport identified for ethylene molecules confined inside a (16, 0) SWCNT at $T = 300$ K. Fickian diffusion is exemplified for a system containing 130 molecules (*bottom curve*, $\rho = 15.751$ mol·L^{-1}), and ballistic transport for a nanotube with 2 molecules (*top curve*, $\rho = 0.242$ mol·L^{-1})

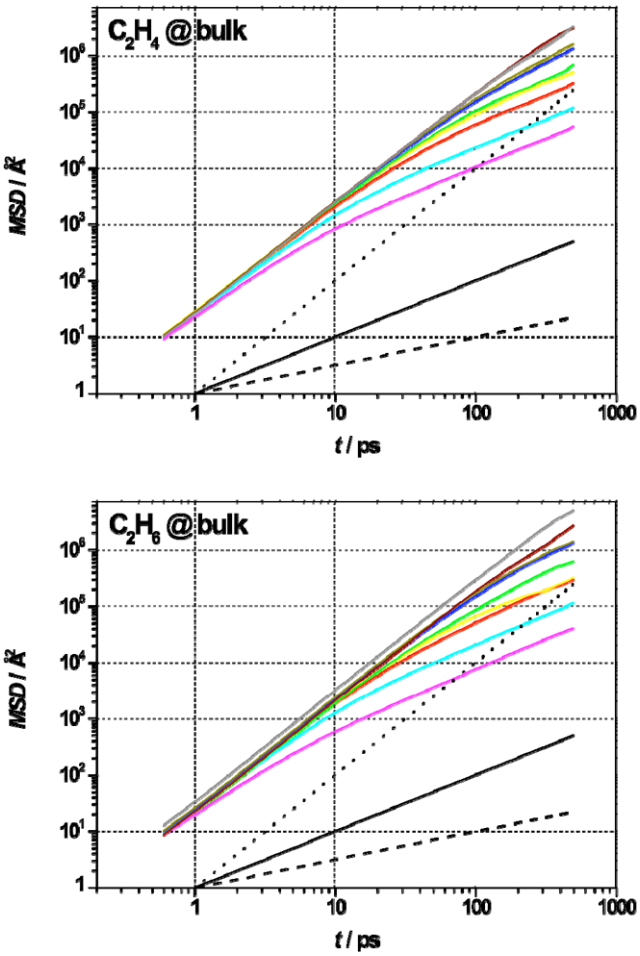

Fig. 3 Plot of the mean-squared displacement, *MSD*, for the bulk fluid phases of ethylene and ethane ($T = 300$ K). Density increases from top to bottom, from 0.026 mol·L^{-1} to 2.969 mol·L^{-1} (C_2H_4) and from 0.011 mol·L^{-1} to 3.711 mol·L^{-1} (C_2H_6) (cf. Table 1). The different diffusion mechanisms are indicated for comparison purposes: ballistic (*dotted*), Fickian (*straight line*) and single-filed (*dashed*)

we have found no evidence of single-file diffusion, in line with findings that have been previously observed for water molecules in narrow armchair tubes (Striolo 2006) and inside zeolites (Jakobtorweihen et al. 2007), and for *n*-alkanes diffusing inside SWCNTs (Krishna and van Baten 2006).

Evaluating the MSD appropriately, involves fitting simulation data to a linear function in the Fickian regime, where $\langle r^2 \rangle$ is linearly proportional to t. Thus, one needs to be aware of the possible existence of an initial transition regime. This issue can be dealt with, arranging the results in a double logarithmic plot (Figs. 3–4), and identifying the region where the corresponding curves exhibit a slope equal to unity (characteristic of Fickian diffusion); in these areas we have calculated self-diffusion coefficients by linear regression of MSD data, using at least 100 ps of simulation time.

4.1 Bulk phases

As described earlier (cf. Sect. 3) we have built simulation boxes with different bulk fluid densities, and the corresponding findings are recorded in Fig. 3. Mean-squared displacement starts as ballistic (proportional to t^2) for all densities studied, and around 10–300 ps a change in the slopes seems to indicate a transition to the Fickian regime. The exact beginning of this transition depends on the bulk fluid density: it starts to occur earlier for the higher density fluid, *ca.* 10 ps (pink), and around 300 ps for the lowest one (gray). For all cases, in the limit $t > 300$ ps, the MSD behavior suggests a Fickian-type curve (proportional to t). If one compares results obtained for different densities, there seems to be a lower limit where Fickian diffusion loses its dominating role, and ballistic transport starts to play a major part. In the case of C_2H_4, this density is located between 0.21 mol·L^{-1} and 0.10 mol·L^{-1}. For fluids with densities less than 0.21 mol·L^{-1}, we can still find local areas of Fickian diffusion, typically for $t > 300$ ps.

The usual general trend is observed, i.e., self-diffusion coefficients increase with decreasing density (Table 1). As this latter property approaches the limit of infinite dilution, molecules become less and less constrained by the environment, and we can observe a dramatic increase in D as density falls bellow 0.2 mol·L^{-1}. This monotonic behavior can be satisfactorily described in the whole density range, correlating the results according to Eq. 2; the fitted parameters A and B thus obtained ($R^2 = 0.995$), are indicated in Table 1,

$$D = A\rho^{-B}. \tag{2}$$

One can test the validity of such an empirical equation, and the underlying molecular potential employed in the simulations by considering C_2H_4 and Eq. 2 with the parameters given in Table 1, to estimate the fluid self-diffusivity at a total bulk density of $\rho = 9.8895$ mol·L^{-1}. At these conditions we obtain a prediction which presents less than 5% deviation in comparison with the experimental data compiled by Fernández et al. (2005).

4.2 Confined fluids

The effect exherted on the fluid's dynamical properties, under confinement within the SWCNT, depends, as might be expected, on the total amount of confined substance (loading capacity). We have analyzed the molecules trajectories and determined the corresponding mean-squared displacement as a function of simulation time for different loadings (Fig. 4). One needs to keep in mind that the highest density systems correspond to a nanopore which is totally filled, as determined in part I (Cruz and Müller 2008).

Generally speaking, the MSD curves of Fig. 4 point out to the existence of two dominant modes of transport in the

Table 1 Self-diffusion coefficients at different bulk phase densities ($T = 300$ K). Constants A and B are the parameters for Eq. 2

Pure C_2H_4		Pure C_2H_6	
ρ (mol·L^{-1})	10^6 D (m^2·s^{-1})	ρ (mol·L^{-1})	10^6 D (m^2·s^{-1})
Pure C_2H_4		Pure C_2H_6	
2.969	0.180 ± 0.001	3.711	0.139 ± 0.001
1.254	0.393 ± 0.003	1.254	0.392 ± 0.003
0.497	1.042 ± 0.009	0.512	0.946 ± 0.016
0.497[a]	0.706 ± 0.009	0.334	1.096 ± 0.014
0.327	1.612 ± 0.017	0.208	1.807 ± 0.063
0.208	1.852 ± 0.017	0.076	5.48 ± 0.07
0.208[a]	1.919 ± 0.017	0.059	5.53 ± 0.14
0.096	5.419 ± 0.085	0.022	15.09 ± 0.15
0.096[a]	4.609 ± 0.058	0.011	21.9 ± 0.1
0.078	6.937 ± 0.024	$A = 4.6909 \times 10^{-7}$ (m^2·s^{-1}·mol^{-1}·L)	
0.078[a]	5.531 ± 0.034	$B = -0.8866$	
0.045	12.40 ± 0.29		
0.026	18.00 ± 0.07		
0.026[a]	14.74 ± 0.21		
$A = 5.0494 \times 10^{-7}$ (m^2·s^{-1}·mol^{-1}·L)			
$B = -0.9959$			

[a]Data for the two-sphere Lennard-Jones dumbbell model with embedded central quadrupole moment (2CLJQ)

long simulation time region ($t > 100$ ps), namely Fickian and ballistic-type. For densities above $\rho = 5.5$ mol·L^{-1}, the systems' dynamical properties seem to be overall governed by Fickian diffusion. Despite some small kinks and/or bumps in the mean-squared displacement curves, they regain an approximately linear behavior with t after those anomalies, assuming an identical slope. For example, in the case of ethane at $\rho = 14.055$ mol·L^{-1} (red line in Fig. 4), this was corroborated by extending the simulation time until 1 ns. Mao et al. identified a mixed mode of transport for very dense ethane inside a (16, 0) SWCNT (Mao and Sinnott 2000), with components from both Fickian and single-file type, but they have concluded that ethylene exhibits normal (Fickian) mode. Their short time scale did not allow them to confirm the persistence of the C_2H_6 mixed behavior after *ca.* 100 ps. The rigid (20, 0) SWCNT simulations of Krishna et al. concluded that for $t > 100$ ps, Fickian is the dominant mode of transport for dense ethane, but also for other n-alkanes up to n-butane (Krishna and van Baten 2006). The low density confined fluids ($\rho < 5.5$ mol·L^{-1}) show a transition behavior between ballistic and Fickian transport, persistent up to 200–300 ps. Beyond this time region, molecular displacement is essentially ballistic in nature, for the MSD curves lose their linear relationship with t and start exhibiting a linear dependence with t^2. Nonetheless, one can identify local regions of Fickian self-diffusion in the mixed mode regime, and estimate the corresponding diffusivities (we have used 50 ps of simulation data to determine D). As a rule of thumb, when density decreases there seems to be a region where the dominant overall mode of transport changes from Fickian self-diffusion to ballistic transport: 5.33 mol·L^{-1} $< \rho <$ 7.75 mol·L^{-1} for C_2H_4, and 4.36 mol·L^{-1} $< \rho <$ 6.18 mol·L^{-1} in the case of C_2H_6. This is not surprising if one bears in mind that in the low density end, molecules have plenty of free available space inside the tube, which means that they can find unobstructed preferential molecular paths and move along them originating a ballistic-type regime.

Results obtained for the self-diffusivities are recorded in Table 2; the fluid mobility inside the nanotube increases approximately linearly with decreasing loading. As we approach the limit of infinite dilution, self-diffusivities start to increase very sharply, reaching limiting values of $D_{ethylene} = 114.6 \times 10^{-8}$ m^2·s^{-1} and $D_{ethane} = 65.5 \times 10^{-8}$ m^2·s^{-1}. The zero-loading limiting behavior of ethane inside a (20, 0) zig-zag SWCNT has been studied using united-atom models for the fluids and rigid frameworks for the nanotube walls. Krishna and van Baten (2006) reported a value of $D^0_{ethane} = 2500 \times 10^8$ m^2·s^{-1} and Jakobtorweihen et al. (2007) of $D^0_{ethane} = 2117 \times 10^8$ m^2·s^{-1}. We can extrapolate data recorded in Table 2 using a correlation model identical to the one employed for the bulk fluids (Eq. 2). At $\rho_{ethane} = 0.025$ mol·L^{-1}, a value of $D^0_{ethane} = 2079 \times 10^8$ m^2·s^{-1} is obtained, in satisfactory agreement with the previous reported results. There are no simulation results studying the behavior of ethylene in the zero-loading limit. Nonetheless, previous studies of the dynamical flow of ethylene and ethane through an 80 Å length (16, 0) SWCNT have reported the axial mean-squared displacement (Mao and Sinnott 2000), neglecting transport in the plane perpendicular

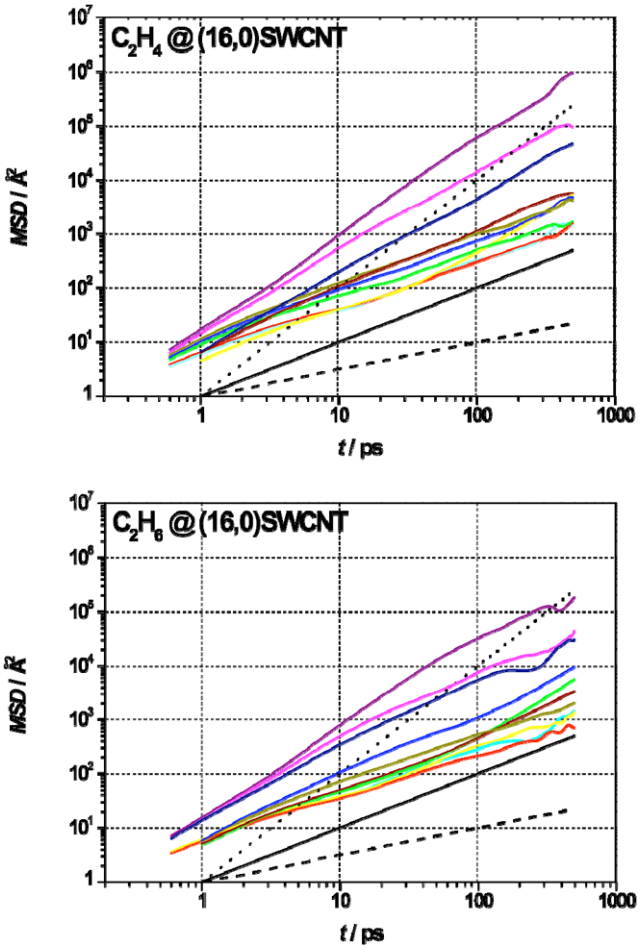

Fig. 4 Plot of the mean-squared displacement, *MSD*, for fluids confined in a (16, 0) zig-zag SWCNT ($T = 300$ K). Density increases *from top to bottom*, respectively, from 0.242 mol·L^{-1} to 15.751 mol·L^{-1} (C_2H_4) and from 0.242 mol·L^{-1} to 14.055 mol·L^{-1} (C_2H_6) (cf. Table 2). The different diffusion mechanisms are indicated for comparison purposes: ballistic (*dotted*), Fickian (*straight line*) and single-filed (*dashed*)

to the tube walls. In such a case, for an (apparent) ethylene density of *ca.* 100 mol·L^{-1}, it was estimated that $D_{ethylene} = 0.981 \times 10^{-8}$ m^2·s^{-1}, roughly in the same order of magnitude as the value now being reported for the highest density system. We have considered explicit electrostatics for the fluid-fluid interactions and a flexible double bond on the ethylene molecule. This may help explaining why our self-diffusivity for dense ethylene is slightly lower. Due to the existence of explicit π–π interactions in the fluid, molecules are able to align themselves according to the direction of the quadrupole moment (Müller 2008), resulting in a "structured" fluid, and thus hindering molecular displacement inside the confining host.

An interesting aspect related to the dynamical behavior of these confined fluids, is the intrinsic effect originating from the nanotube geometry. The confinement of liquid ethane onto carbon slit pores of different widths has been studied before (Klochko et al. 1999). The weighted average (Coasne et al. 2006) self-diffusion coefficients for graphite slit pores of pore widths of 11.7 Å and 26.8 Å, corresponds to $D_{ethane} = 1.62 \times 10^{-9}$ m^2·s^{-1} and $D_{ethane} = 2.19 \times 10^{-9}$ m^2·s^{-1}. Even for the largest slit pore width (roughly three times larger than the diameters of the nanotubes considered here, *cf.* Sect. 2), the diffusivity is two orders of magnitude lower than that within a cylindrical SWCNT. Further comparisons are needed to generalize these observations. Although molecular dynamics simulations with C_2H_6 have also been performed in zeolitic confining cages, results are not straightforwardly comparable with ours as ethane molecules have been modeled as rigid diatomics diffusing along a 7.3 Å diameter pore (Adhangale and Keffer 2002).

Previous molecular simulation studies have suggested that nanotube topology is a relatively unimportant factor affecting confined molecular displacement. It has been verified for water inside zig-zag, chiral and armchair tubes (Alexiadis and Kassinos 2008), for methane, ethylene and ethane confined in zig-zag and armchair symmetries (Mao and Sinnott 2000, 2002) and in a binary mixture of CH_4/C_2H_6 (Mao and Sinnott 2001). Results recorded in Table 2 seem to corroborate this idea, and, in the case of ethane and ethylene, extend the validity of such findings for chiral SWCNTs. In fact, when both fluids are confined inside nanotubes of different topology, the most important difference in their self-diffusivities seems to arise from the nanotube loading (density), and not from the specific symmetry.

It is important to point out, however, that the extent of this conclusion depends on the level of detail that is sought. Considering the level of uncertainty associated with the calculation of diffusion coefficients and the orders of magnitude of difference between reported values, sometimes due to small changes in the potentials or conditions (c.f. Table 2) it is understandable that the difference in diffusivities due to chirality be overlooked. An exemplary work that produces an apparently conflicting result has recently been published (Liu et al. 2008). There, the authors note that the difference in potential energy surfaces inside the nanotubes induces different diffusion coefficients. As they clearly show, the chirality differences amongst the nanotubes, produce different plausible mean paths for the molecules which move close to the walls. Particularly, zig-zag nanotubes will have a minimum energy path which spirals along the axis of the tube, much akin to the bores inside a rifle. Armchair nanotubes will have minimum energy paths that are aligned with the tube axis. For very low loadings, molecules may preferentially follow these minimum energy paths close to the walls, inducing effectively different diffusivities. In the electronic supplementary material we present a movie that showcases this spiral mode of transport, previously reported by (Mao and Sinnott 2002). At higher loadings, these differences seem to be overcome by the general collisions amongst adsorbed molecules.

Table 2 Self-diffusion coefficients for C_2H_4 and C_2H_6 at different loadings, confined inside zig-zag (16, 0), chiral (12, 6) and armchair (9, 9) SWCNTs ($T = 300$ K)[a,b]

Pure C_2H_4		Pure C_2H_6	
ρ (mol·L^{-1})	10^6 D (m^2·s^{-1})	ρ (mol·L^{-1})	10^6 D (m^2·s^{-1})
15.751	0.340 ± 0.009	14.055	0.269 ± 0.009
16.159$^{(12,6)}$	0.670 ± 0.011	13.833	0.419 ± 0.007
17.166$^{(9,9)}$	0.930 ± 0.051	14.419$^{(12,6)}$	0.247 ± 0.013
15.024	0.411 ± 0.006	15.318$^{(9,9)}$	0.257 ± 0.008
15.024[c]	0.411 ± 0.006	13.207	0.468 ± 0.012
13.086	0.728 ± 0.014	9.208	0.764 ± 0.035
10.905	0.773 ± 0.036	8.724	0.585 ± 0.009
8.966	1.422 ± 0.027	6.179	1.046 ± 0.019
8.966[c]	0.723 ± 0.010	4.362	2.05 ± 0.16
7.754	1.494 ± 0.018	4.475$^{(12,6)}$	1.349 ± 0.091
5.331	1.813 ± 0.033	4.754$^{(9,9)}$	2.196 ± 0.048
5.469$^{(12,6)}$	2.864 ± 0.044	2.239	9.59 ± 0.21
5.810$^{(9,9)}$	2.207 ± 0.065	1.090	14.39 ± 0.56
2.423	4.585 ± 0.048	0.242	65.5 ± 0.355
2.423[c]	2.95 ± 0.15		
1.212	25.5 ± 1.4		
0.242	114.6 ± 8.2		
0.242[c]	36.19 ± 3.8		

[a]Labels (12, 6) and (9, 9) represent the chiral and armchair nanotubes, respectively

[b]For the lower density systems, $\rho < 5.5$ mol·L^{-1}, self-diffusion coefficients were estimated from local Fickian regions (see text for details)

[c]Data for the two-sphere Lennard-Jones dumbbell model with embedded central quadrupole moment (2CLJQ)

Recently, Mittal et al. (2007), improving on Rosenfeld's (1977, 1999) and Dzugutov's (1996, 2002) pioneer work, presented a detailed analysis on the dependence between self-diffusivities and static thermodynamic properties such as density and excess entropy. Using the Lennard-Jones potential and a monoatomic model for the fluid, they suggested a direct relationship (scaling law) between self-diffusivity and an effective packing fraction, which allows both bulk fluid and confined phase self-diffusion data to collapse onto the same curve. In their definition of packing fraction, the confined volume has been calculated based on the distance between particle surfaces of the confined space (instead of the distance between particle centers). Their findings suggest that confined phase diffusion data could be estimated by the knowledge of the corresponding bulk fluid structural properties, and this idea can become immediately appealing when one keeps in mind practical and industrial applications. If we plot our diffusion data according to Mittal's idea of a "master curve", the result is somehow surprising (Fig. 5), for in the present work, C_2H_4 and C_2H_6 have been modeled as polyatomic flexible molecules.

One can observe that in spite of some clear deviations, data from the inhomogeneous systems roughly collapse onto the same general trend observed for the bulk phase results. In other words, loading effects (density) seem to determine in the same way the diffusion within the bulk phase, and in the confined systems.

In the previous paper of this series (Cruz and Müller 2008) we showed that a fine description of the fluid molecules, in terms of a fully atomistic intermolecular potential model, as opposed to a simpler coarse-grained united-atom model, captured some effects which otherwise would be lost when describing the adsorption on nanotubes. In Fig. 5 we additionally plot results obtained by using a two-sphere Lennard-Jones dumbbell model with embedded central quadrupole moment (2CLJQ), as described previously (Cruz and Müller 2008). While the overall trends in values in both the bulk and confined fluid are retained, a consistent shift towards lower diffusivities is seen. As with the adsorption results, at higher densities, the differences between the atomistic and the coarse grained model become less apparent.

5 Conclusions

Dynamical properties of C_2H_4 and C_2H_6, both in the bulk fluid phase and confined inside SWCNTs of different symmetries, have been investigated at $T = 300$ K, and densities of 0.026 mol·L^{-1} $< \rho <$ 15.751 mol·L^{-1} and 0.011 mol·L^{-1} $< \rho <$ 14.055 mol·L^{-1}, respectively. From the MSD curves, as expected, we observed a monotonical decrease of the self-diffusion coefficient with increasing density. For the bulk fluids, an empirical correlation (Eq. 1) has been established that enabled direct comparison with experimental data; in the case of ethylene, discrepancies were found to be less than 5% up to $\rho \approx 10$ mol·L^{-1}. Upon confinement inside a SWCNT, nanotube topology seems to be

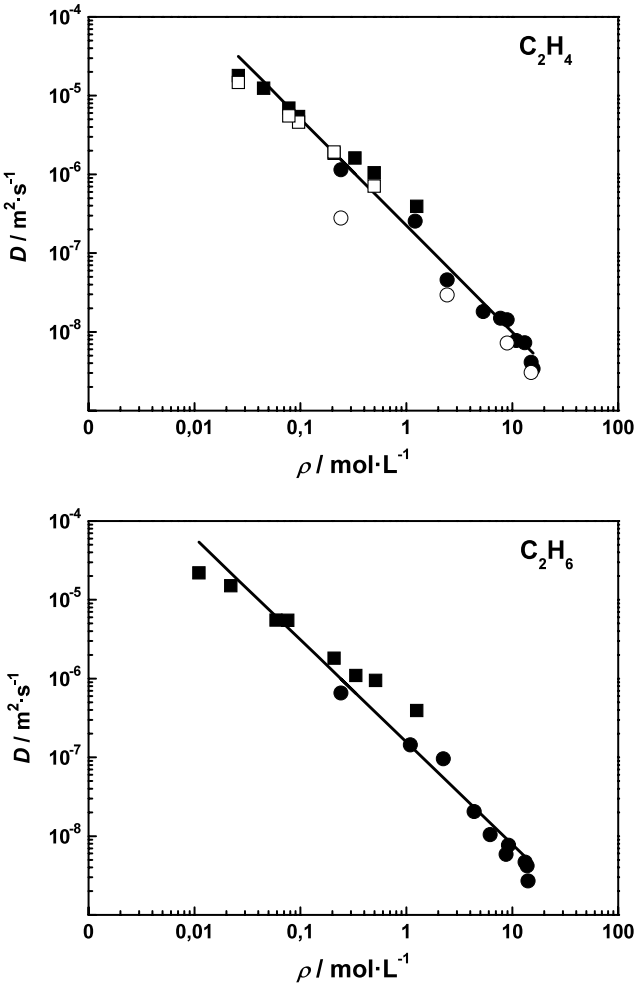

Fig. 5 Self-diffusivity versus molecular density, for the bulk (*squares*) and a fluid confined in a (16, 0) SWCNT (*circles*) at $T = 300$ K. *Solid symbols* correspond to the AA-OPLS potential, while *open symbols* correspond to the coarse-grained two center Lennard-Jones dumbbells with central quadrupole moment (2CLJQ). *Lines* are a guide to the eye

a relatively unimportant factor influencing the molecules' dynamics. Simulations conducted for zig-zag (16, 0), chiral (12, 6) and armchair (9, 9) tubes, at high densities and close to the zero-loading limit, did not detect a significant difference in the corresponding self-diffusion coefficients. The high-density systems confined onto a zig-zag lattice, usually exhibited a dominant Fickian-type mode of transport, although a transition seems to occur for molecular densities $\rho < 5.5$ mol·L^{-1}. Below this threshold, molecules moved with a mixed mode transport, combining components from Fickian and ballistic diffusion.

In all cases studied and at a given density, the diffusivities of ethylene are larger than those of ethane, although the difference is relatively minor. In our previous work we found that ethane is the preferred adsorbed species, again by a marginal amount. The enhanced diffusivity of ethylene is expected to hamper the prospects of using nanotubes as effective separation agents for the ethylene/ethane mixtures.

Pore loading seems to be the governing factor as far as dynamical properties are concerned. The collapse into a single "master curve" of self-diffusivity data obtained in the bulk phase and in the confining host, corroborates the density scaling law previously observed for monoatomic and dense Lennard-Jones fluids, opening the possibility of estimating the fluid dynamical behavior from its statical, and easily accessible, molecular density.

Acknowledgements This work has been supported by the Engineering and Physical Sciences Research Council of the U.K. through Grant EP/D035171/1.

References

Adhangale, P., Keffer, D.: Single-file motion of polyatomic molecules in one-dimensional nanoporous materials. Mol. Phys. **100**, 2727–2733 (2002)

Alexiadis, A., Kassinos, S.: The density of water in carbon nanotubes. Chem. Eng. Sci. (2008)

Allen, M.P., Tildesley, D.J.: Computer Simulation of Liquids. Clarendon, Oxford (1990)

Arora, G., Sandler, S.I.: Nanoporous carbon membranes for separation of nitrogen and oxygen: insight from molecular simulations. Fluid Phase Equilib. **259**, 3–8 (2007)

Bhatia, S.K., Chen, H., Sholl, D.S.: Comparisons of diffusive and viscous contributions to transport coefficients of light gases in single-walled carbon nanotubes. Mol. Simul. **31**, 643–649 (2005)

Cao, D., Wu, J.: Self-diffusion of methane in single-walled carbon nanotubes at sub- and supercritical conditions. Langmuir **20**, 3759–3765 (2004)

Chen, H., Sholl, D.S.: Rapid diffusion of CH4/H2 mixtures in single-walled carbon nanotubes. J. Am. Chem. Soc. **126**, 7778–7779 (2004)

Chen, H., Sholl, D.S.: Predictions of selectivity and flux for CH_4/H_2 separations using single salled carbon nanotubes as membranes. J. Memb. Sci. **269**, 152–160 (2006)

Chen, H., Johnson, J.K., Sholl, D.S.: Transport diffusion of gases is rapid in flexible carbon nanotubes. J. Phys. Chem. B **110**, 1971–1975 (2006)

Coasne, B., Jain, S.K., Gubbins, K.E.: Adsorption, structure and dynamics of fluids in ordered and disordered models of porous carbons. Mol. Phys. **104**, 3491–3499 (2006)

Corry, B.: Designing carbon nanotube membranes for efficient water desalination. J. Phys. Chem. B **112**, 1427–1434 (2009)

Cruz, F.J.A.L., Müller, E.A.: Behavior of ethylene/ethane binary mixtures within single-walled carbon nanotubes, 1: adsorption and equilibrium properties. Adsorption (2008, submitted)

Dubbeldam, D., Beerdsen, E., Vlugt, T.J.H., Smit, B.: Molecular simulation of loading-dependent diffusion in nanoporous materials using extended dynamically corrected transition state theory. J. Chem. Phys. **122**, 224712 (2005)

Düren, T., Keil, F.J., Seaton, N.A.: Molecular simulation of adsorption and transport diffusion of model fluids in carbon nanotubes. Mol. Phys. **100**, 3741–3751 (2002)

Dzugutov, M.: A Universal scaling law for atomic diffusion in condensed matter. Nature **381**, 137–139 (1996)

Dzugutov, M.: Anomalous slowing down in the metastable liquid of hard spheres. Phys. Rev. E **65**, 032501 (2002)

Fernández, G.A., Vrabec, J., Hasse, H.: Self-diffusion and binary Maxwell–Stefan diffusion coefficients of quadrupolar real fluids from molecular simulation. Int. J. Therm. **26**, 1389–1407 (2005)

Gelb, L.D., Gubbins, K.E., Radhakrishnan, R., Sliwinska-Bartkowiak, M.: Phase separation in confined systems. Rep. Prog. Phys. **62**, 1573–1659 (1999)

Haile, J.M.: Molecular Dynamics Simulation: Elementary Methods. Wiley, New York (1992)

Jakobtorweihen, S., Keil, F.J., Smit, B.: Temperature and size effects on diffusion in carbon nanotubes. J. Phys. Chem. B **110**, 16332–16336 (2006)

Jakobtorweihen, S., Lowe, C.P., Keil, F.J., Smit, B.: Diffusion of chain molecules and mixtures in carbon nanotubes: the effect of host lattice flexibility and theory of diffusion in the Knudsen regime. J. Chem. Phys. **127**, 24904 (2007)

Jorgensen, W.L., Maxwell, D.S., Tirado-Rives, J.: Development and testing of the OPLS all-atom force field on conformational energetics and properties of organic liquids. J. Am. Chem. Soc. **118**, 11225–11236 (1996)

Kaneko, K., Cracknell, R.F., Nicholson, D.: Nitrogen adsorption in slit pores at ambient temperatures: comparison of simulation and experiment. Langmuir **10**, 4506–4609 (1994)

Klochko, A.V., Brodskaya, E.N., Piotrovskaya, E.M.: Computer simulations of dependence of adsorption characteristics of ethane on the size of graphite micropores. Langmuir **15**, 545–552 (1999)

Krishna, R., van Baten, J.M.: Describing binary mixture diffusion in carbon nanotubes with the Maxwell-Stefan equations. An investigation using molecular dynamics simulations. Fluid Phase Equilib. **45**, 2084–2093 (2006)

Leroy, F., Rousseau, B., Fuchs, A.H.: Self-diffusion of *n*-alkanes in silicalite using molecular dynamics simulation: a comparison between rigid and flexible frameworks. Phys. Chem. Chem. Phys. **6**, 775–783 (2004)

Liu, Y.-C., Shen, J.-W., Gubbins, K.E., Moore, J.D., Wu, T., Wang, Q.: Diffusion dynamics of water controlled by topology of potential energy surface inside carbon nanotubes. Phys. Rev. B **77**, 125438 (2008)

Majumder, M., Chopra, N., Andrews, R., Hinds, B.J.: Nanoscale hydrodynamics: enhanced flow in carbon nanotubes. Nature **438**, 44 (2006)

Mao, Z., Sinnott, S.B.: A Computational study of molecular diffusion and dynamic flow through carbon nanotubes. J. Phys. Chem. B **104**, 4618 (2000)

Mao, Z., Sinnott, S.B.: Separation of organic molecular mixtures in carbon nanotubes and bundles: molecular dynamics simulations. J. Phys. Chem. B **105**, 6916–6924 (2001)

Mao, Z., Sinnott, S.B.: Predictions of a spiral diffusion path for nonspherical organic molecules in carbon nanotubes. Phys. Rev. Lett. **89**, 278301 (2002)

McDonald, N.A., Carlson, H.A., Jorgensen, W.L.: Free energies of solvation in chloroform and water from a linear response approach. J. Phys. Org. Chem. **10**, 563–576 (1997)

Meyyappan, M.: Carbon Nanotubes: Science and Applications. CRC Press, London (2005)

Mittal, J., Errington, J.R., Truskett, T.M.: Relationships between self-diffusivity, packing fraction, and excess entropy in simple bulk and confined fluids. J. Phys. Chem. B **111**, 10054–10063 (2007)

Mon, K.K., Percus, J.K.: Self-diffusion of fluids in narrow cylindrical pores. J. Chem. Phys. **117**, 2289–2292 (2002)

Müller, E.A.: Staggered alignment of quadrupolar molecules inside carbon nanotubes. J. Phys. Chem. B **112**, 8999–9005 (2008)

Mukherjee, B., Maiti, P.K., Dasgupta, C., Sood, A.K.: Strong correlations and Fickian water diffusion in narrow carbon nanotubes. J. Chem. Phys. **126**, 124704–124711 (2007)

Nosé, S.: A unified formulation of the constant temperature molecular dynamics methods. J. Chem. Phys. **81**, 511–519 (1984)

Ohba, T., Kaneko, K.: Internal surface area evaluation of carbon nanotube with GCMC simulation-assisted N_2 adsorption. J. Phys. Chem. B **106**, 7171–7176 (2002)

Rosenfeld, Y.: Relation between the transport coefficients and the internal entropy of simple systems. Phys. Rev. A **15**, 2545–2549 (1977)

Rosenfeld, Y.: A quasi-universal scaling law for atomic transport in simple fluids. J. Phys.: Condens. Matter **11**, 5415–5427 (1999)

Rouquerol, F., Rouquerol, J., Sing, K.: Adsorption by Powders and Porous Media. Academic Press, New York (1998)

Rowlinson, J.S., Swinton, F.L.: Liquids and Liquid Mixtures. Butterworths, London (1982)

Sholl, D.S., Johnson, J.K.: Making high-flux membranes with carbon nanotubes. Science **312**, 1003–1004 (2006)

Skoulidas, A.I., Sholl, D.S., Johnson, J.K.: Adsorption and diffusion of carbon dioxide and nitrogen through single-walled carbon nanotube membranes. J. Chem. Phys. **124**, 54701–54707 (2006)

Smith, W., Todorov, I.T.: A short description of DL_POLY. Mol. Simul. **32**, 935–943 (2006)

Steele, W.A.: The physical interactions of gases with crystalline solids. Surf. Sci. **36**, 317–352 (1973)

Steele, W.A.: The Interaction of Gases with Solid Surfaces. Pergamon, Oxford (1974)

Steele, W.A.: Molecular interactions for physical adsorption. Chem. Rev. **93**, 2355–2378 (1993)

Striolo, A.: The mechanism of water diffusion in narrow carbon nanotubes. Nano Lett. **6**, 633–639 (2006)

Striolo, A.: Water self-diffusion through narrow oxygenated carbon nanotubes. Nanotechnology **18**, 475704–475713 (2007)

Striolo, A., McCabe, C., Cummings, P.T.: Thermodynamic and transport properties of polyhedral oligomeric sislesquioxanes in poly(dimethylsiloxane). J. Phys. Chem. B **109**, 14300 (2005)

Valiullin, R., Naumov, S., Galvosas, P., Karger, J., Woo, H.-J., Porcheron, F., Monson, P.A.: Exploration of molecular dynamics during transient sorption of fluids in mesoporous materials. Nature **443**, 965–968 (2006)

van Gunsteren, W.F., Berendsen, H.J.C.: Computer simulation of molecular dynamics: methodology, applications, and perspectives in chemistry. Angew. Chem. Int. Ed. Engl. **29**, 992–1023 (1990)

Verlet, L.: Computer "experiments" on classical fluids. Thermodynamical properties of Lennard-Jones molecules. Phys. Rev. **159**, 98–103 (1967)

Woodcock, L.V., Singer, K.: Thermodynamics and structural properties of liquid ionic salts obtained by Monte Carlo computation. Trans. Faraday Soc. **67**, 12–30 (1971)

Zimmermann, N.E.R., Jakobtorweihen, S., Beerdsen, E., Smit, B., Keil, F.J.: In-depth study of the influence of host-framework flexibility on the diffusion of small gas molecules in one-dimensional zeolitic pore systems. J. Phys. Chem. C **111**, 17370–17381 (2007)